General Disclaimer

One or more of the Following Statements may affect this Document

- This document has been reproduced from the best copy furnished by the organizational source. It is being released in the interest of making available as much information as possible.

- This document may contain data, which exceeds the sheet parameters. It was furnished in this condition by the organizational source and is the best copy available.

- This document may contain tone-on-tone or color graphs, charts and/or pictures, which have been reproduced in black and white.

- This document is paginated as submitted by the original source.

- Portions of this document are not fully legible due to the historical nature of some of the material. However, it is the best reproduction available from the original submission.

NASA TECHNICAL MEMORANDUM

NASA TM X- 73,169

NASA TM X-73,169

SCANNING LASER-VELOCIMETER SURVEYS AND ANALYSIS OF MULTIPLE VORTEX WAKES OF AN AIRCRAFT

Victor R. Corsiglia and Kenneth L. Orloff

Ames Research Center
Moffett Field, Calif. 94035

August 1976

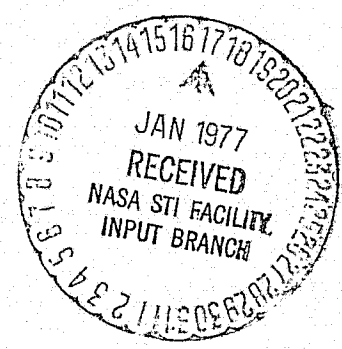

1. Report No.	2. Government Accession No.	3. Recipient's Catalog No.
NASA TM X-73,169		

4. Title and Subtitle	5. Report Date
SCANNING LASER-VELOCIMETER SURVEYS AND ANALYSIS OF MULTIPLE VORTEX WAKES OF AN AIRCRAFT	6. Performing Organization Code

7. Author(s)	8. Performing Organization Report No.
Victor R. Corsiglia and Kenneth L. Orloff	A – 6750
	10. Work Unit No. 514 – 52 – 01
9. Performing Organization Name and Address	11. Contract or Grant No.
Ames Research Center Moffett Field, Calif. 94035	
	13. Type of Report and Period Covered
12. Sponsoring Agency Name and Address	Technical Memorandum
National Aeronautics and Space Administration Washington, D.C. 20546	14. Sponsoring Agency Code

15. Supplementary Notes

16. Abstract

A laser velocimeter capable of rapidly scanning a flow field while simultaneously sensing two components of the velocity was used to measure the vertical and streamwise velocity structure 1.5 spans downstream in the wake of a model typical of a large subsonic transport (Boeing 747). This flow field was modeled by a superposition of axisymmetric vortices with finite cores. This theoretical model was found to agree with the measured velocities everywhere except where two vortices were in close proximity. Vortex strengths derived from the span loading on the wing as predicted by vortex-lattice theory also agree with the present measurements. It was, therefore, concluded that the axisymmetric vortex model used herein is a useful tool for analytically investigating the vortex wakes of aircraft.

17. Key Words (Suggested by Author(s))	18. Distribution Statement
Multiple vortex wakes Laser velocimeter measurements Wake vortex modeling	Unlimited STAR Category – 02

19. Security Classif. (of this report)	20. Security Classif. (of this page)	21. No. of Pages	22. Price*
Unclassified	Unclassified	33	$3.75

*For sale by the National Technical Information Service, Springfield, Virginia 22161

NOTATION

AR	aspect ratio, $\frac{b^2}{S}$
b	wingspan
c	wing chord
$\bar{c}$	average chord, $\frac{s}{b}$
c_ℓ	local lift coefficient, $\frac{dL/dy}{q\bar{c}}$
C_L	total lift coefficient, $\frac{L}{qs}$
f	frequency
L	lift
q	$\frac{1}{2}\rho V_\infty^2$
r	radius from center of vortex
S	wing area
U	streamwise velocity component, positive downstream
V	velocity
V_θ	swirl velocity component
V_∞	free-stream velocity
W	vertical velocity component
x,y,z	coordinate axis: x (positive downstream), y (positive out right wing)
$\bar{x},\bar{y},\bar{z}$,	coordinate axis nondimensionalized by semispan, $\frac{b}{2}$
α	angle of attack
β	laser tilt angle to obtain directional sensitivity
Γ	circulation
$\bar{\Gamma}$	nondimensional circulation, $\frac{\Gamma}{bV_\infty}$
λ	wavelength of light, $\lambda_B = 0.488\ \mu m$, $\lambda_G = 0.5145\ \mu m$
θ	laser beam intersection angle
ρ	air density

Subscripts

B	blue color channel of laser velocimeter
G	green color channel of laser velocimeter

SCANNING LASER-VELOCIMETER SURVEYS AND ANALYSIS OF MULTIPLE VORTEX WAKES OF AN AIRCRAFT

Victor R. Corsiglia and Kenneth L. Orloff

SUMMARY

A laser velocimeter capable of rapidly scanning a flow field while simultaneously sensing two components of the velocity was used to measure the vertical and streamwise velocity structure 1.5 spans downstream in the wake of a model typical of a large subsonic transport (Boeing 747). This flow field was modeled by a superposition of axisymmetric vortices with finite cores. This theoretical model was found to agree with the measured velocities everywhere except where two vortices were in close proximity. Vortex strengths derived from the span loading on the wing as predicted by vortex-lattice theory also agree with the present measurements. It was, therefore, concluded that the axisymmetric vortex model used herein is a useful tool for analytically investigating the vortex wakes of aircraft.

INTRODUCTION

Trailing vortex wakes of large aircraft are a hazard to smaller following aircraft. As a result, the separation distances during landing and take-off that must be imposed to maintain safety are now a determining factor in maximizing runway utilization (ref. 1). Future increases in airport capacity are, therefore, limited by required separations between aircraft due to vortices. In recent years, NASA has conducted considerable research into reducing the wake of large aircraft by aerodynamic means (ref. 2). As a result of this research, several techniques have been found to be effective in deintensifying the wake. One of these techniques is to configure the aircraft so that it sheds multiple vortices from the wing in such a way that these vortices interact and merge (ref. 3). A particular configuration that employs this technique is the B747 airplane with the inboard trailing-edge flaps set to the landing position and the outboard trailing-edge flaps retracted (ref. 4). Recent flow visualization studies conducted on various configurations of this aircraft have shown the trajectories of vortices in the wake (ref. 5). The objective of the present study was to measure the velocity distributions in the wake and to determine the size and strength of each of the vortices. A second objective was to investigate the effect of the landing gear on the wake, because it had been found in flight and ground-based tests that, at downstream distances greater than about 30 spans, lowering the landing gear intensified the wake (refs. 6 and 7).

In an earlier investigation using a rotating-arm hot-wire anemometer (ref. 8), the flow field was scanned rapidly along the arc of a circle that passed very near a vortex core. This technique was shown to be effective for the case of simple wakes where only a single vortex pair existed. When this technique was applied to a complex wake involving multiple vortices per side, difficulty was encountered in interpreting the measured results because insufficient data were available to adequately define the various wake vortices. In the present study, an improved technique for the case of complex wakes was used. The flow field was scanned rapidly in the lateral direction at successive vertical locations. Data were accumulated in the vicinity of each vortex to provide more information about the flow as compared to the rotating arm technique. Furthermore, the present measurements were made with a laser velocimeter, which assured that the measuring device did not interfere with the flow field.

The present paper presents the results (obtained by means of a scanning, two-dimensional laser velocimeter) of velocity surveys made in the Ames 7- by 10-Foot Wind Tunnel at 1.5 spans downstream from the generator model. The strengths of the various vortices in the wake were determined by use of a theoretical axisymmetric model for the swirl component of velocity for each vortex. Comparisons are shown between the measurements and this axisymmetric model. An earlier paper (ref. 9) describes the apparatus, instrumentation, and the signal processing technique, and shows some sample results from the present tests.

MODEL AND INSTRUMENTATION

The model that was used to generate the vortices was mounted inverted on a single strut at the forward end of the test section (fig. 2 of ref. 9). This mounting provided maximum downstream distance and minimum interference between the strut wake and the wing wake. Angle of attack was varied by adjusting the clevis pivot at the top of the strut. Details of the model, which was identical to that used in earlier studies (ref. 4), appear in figure 1 and table 1. Two configurations of trailing-edge flap were used in the present studies. In one configuration, both the inboard and outboard trailing-edge flaps were set to the landing setting (herein labeled 30°/30°). In the other configuration, the inboard flap deflection was the same, but the outboard flap was set to the zero setting (labeled 30°/0°). The wind-tunnel and test conditions also appear in table 1.

The laser beams passed through the side window of the wind tunnel to the measuring point, which is indicated by the crossing of the beams (fig. 2 of ref. 9). The velocimeter was capable of scanning this measuring point laterally across the tunnel test section over about 2 m in 3 sec. Both the vertical and streamwise components of velocity were simultaneously measured by arranging an orthogonal array of crossed beams in two colors that were available from the laser. Directional sensitivity was obtained by tilting the laser unit approximately 40° so that both laser channels included a free-stream velocity component and, therefore, did not change in velocity direction. The laser velocimeter is further described in references 9 and 10. Details of the signal processing technique used in the present tests are contained in reference 9. Lift coefficient data were obtained by measuring the lift with a strain-gage balance and the dynamic pressure with a pitot-static tube.

DATA REDUCTION AND ANALYSIS

The measured modulation frequency of the scattered laser light and the laser cross beam angle were converted to velocity by the following expressions:

Velocity normal to the interference fringes:

$$V_B = \frac{f_B \lambda_B}{2 \sin \theta/2} \qquad V_G = \frac{f_G \lambda_G}{2 \sin \theta/2}$$

where subscripts B and G refer to the blue and green color channels, respectively, of the laser velocimeter. The laser cross beam angle, θ, which varied across the test section, was calibrated by measuring the beam spacing and the distance to the window of the wind tunnel from the focal point.

Vertical and streamwise velocity:

$$U = V_B \sin \beta + V_G \cos \beta$$

$$W = V_B \cos\beta - V_G \sin\beta$$

where β is the laser tilt angle that was used to provide directional sensitivity. Samples of data records and a processed plot for the vertical and streamwise velocity appear in reference 9. The computed velocities were smoothed by removing obviously bad points which were due to frequency tracker dropout (see ref. 9), and by locally least square fairing the data to a polynomial. Figure 2 contains a typical smoothed data plot.

Analysis

The measured velocity flow field was modeled by superposition of axisymmetric vortices with finite cores. First, it was necessary to locate the centers of vorticity by locating an axial velocity defect coupled with swirl-like vertical velocity. (The location of the vortices for a particular configuration was approximately known from flow visualization (fig. 3 of ref. 9) and from earlier flow visualization studies (ref. 5).) The first iteration for determining the strength of the vortices was made by using point vortices to match the velocities from the theoretical model with the measured velocities. The circulation distribution in the vicinity of each vortex center was then obtained by first subtracting the vertical component of velocity of all the other vortices in the wake along a horizontal line passing through the vortex center, and then computing the circulation of the unknown vortex from the following expression:

$$\Gamma = 2\pi r\, V_\theta$$

where V_θ was set equal to the measured vertical velocity corrected for the induced velocity of all of the other vortices in the flow field.

RESULTS AND DISCUSSION

Effect of Landing Gear

An investigation was made to measure the effect of the landing gear on the wake behind the 30°/0° configuration. The lateral distribution of the vertical velocity component is shown on figure 3 for various lateral passes through the wake. These plots were made from smoothed data plots similar to the one shown on figure 2. Comparison of the velocities between landing gear up and down for all of the vertical locations indicates that no significant effect of the landing gear is apparent. However, an investigation of the streamwise velocity component (not presented here) did indicate a streamwise velocity defect in the wake due to the landing gear. It was, therefore, concluded that the wake vertical velocities at 1.5 spans downstream are only slightly affected by the landing gear and that the reduced alleviation found in earlier investigations at over 30 spans downstream (ref. 6) does not manifest itself until further downstream than 1.5 spans.

Analysis of Wake Velocities

Vortex locations – Vortices for the two configurations used in the present study are shed from each flap edge as well as the wing tip (fig. 4). Furthermore, there are vortices shed from the horizontal stabilizer (not shown). Downstream from the generator at distances greater than about 13 spans, the vortices merge into a single pair that is diffuse for the 30°/0° configuration and

concentrated for the 30°/30° configuration. At 1.5 spans downstream, the various vortices have not yet completed their merge, so that as many as four and six vortices per side would be expected for the 30°/0° and 30°/30° configurations, respectively.

The vortex locations were determined by matching the measured vertical and streamwise velocity components with the axial and rotational properties of vortices near their center; that is, when a lateral scan was made through a vortex center, a swirl-like vertical velocity component coupled with a defect in the streamwise velocity component would occur. As shown in figure 5, for $\bar{z} = -0.38$, the horizontal scan went directly through the center of the flap outboard vortex. At a slightly greater distance below the wing lower surface ($\bar{z} = -0.44$), the scan went through the center of the vortex shed by the inboard edge of the flap. The presence of the nearby outboard flap vortex, however, also strongly affects the vertical velocity. Similarly, the wing-tip vortex was found above the wing upper surface ($\bar{z} = 0.17$). The streamwise velocity defect associated with each vortex occurs most prominently near the vortex center and helps to locate the various vortices at each vertical location.

Circulation distribution, 30°/0° – The foregoing procedure was used to determine the distribution of vorticity within each vortex shed by the 30°/0° configuration. The vortex locations, strengths, and distributions of circulation are shown on figures 6 and 7. When all four of the vortices in the wake are included in the theoretical model, good agreement is achieved with the measurements for a wide range of vertical locations. The sensitivity of the agreement between the wake model and the measured data was emphasized by the velocity field of the vortex from the horizontal tail (vortex 4 in fig. 6). The flow was first modeled by using only the three vortices from the wing, because the tail vortex was believed to be too weak to appreciably influence the wake structure. However, it was not until all four vortices were included in the model that the agreement in figure 8 could be achieved (e.g., see fig. 8 for locations $\bar{z} = -0.408$ and -0.359). In some of the horizontal traverses, it was found that the agreement could be improved by using a slightly different value of $\bar{z}$ in the theoretical model (see fig. 8, $\bar{z} = -0.294$ and -0.246). This is the result of the slight meander of the vortices in the wind tunnel. Although each horizontal scan was made rapidly to avoid the effects of meander, the time between successive vertical locations was large and at nonuniform increments. However, since the meander at the 1.5-span downstream station for these tests was much less than reported by the present author for the considerably greater downstream distance used in earlier tests (ref. 8), a steady-state model could be deduced from the present test data.

Circulation distributions, 30°/30° – Figure 9 shows the region of significant measured streamwise velocity defect along with the measured locations of the vortices. The theoretical vortex strengths and distributions are presented in figures 10 and 11. A much more complex wake than the 30°/0° configuration, containing six vortices per side, was found. The strengths and distributions of circulation were fairly easy to obtain for the 30°/0° configuration. However, for the 30°/30° configuration, the analysis became quite tedious because of the large number of closely spaced vortices. The analysis could be expedited for this type of configuration by simultaneously evaluating (with a least square curve fit procedure) all of the vortex strengths. Such a procedure is now being developed by NEAR, Inc.* Once again, good agreement between the theoretical model and the measurements was found everywhere except for a consistent trend to underpredict for $\bar{y}$ greater than 0.8 (fig. 12). Vortices 3 and 5 are overlapping in this region (fig. 10). Modeling the flow as the sum of axisymmetric vortices appears to be inadequate in the overlap regions. Also, the $\bar{\Gamma}$ vs $\bar{r}$ distribution was found to be similar for all of the vortices analyzed

*Under contract to Ames Research Center.

except vortex 5 (fig. 11). The unusual shape of this curve may be the result of using an axisymmetric model for vortices undergoing a merger process. Computations of the details of vortex merging (ref. 3) indicate that the interactions of closely spaced vortices can lead to highly noncircular shapes; this finding tends to confirm the foregoing conjecture.

Comparison with vortex-lattice theory – The strengths of the wing vortices were estimated from a span loading which was calculated by use of a vortex-lattice theory developed by Hough (ref. 11). The way in which the span loading for the two configurations is divided to determine the strengths of the vortices from the wing is indicated in figure 13 (vortex numbers correspond to the numbers used on figs. 6 and 10). The vortex strength is related to the span loading by the expression:

$$\bar{\Gamma} = \frac{C_L}{2AR} \frac{c_\ell c}{C_L \bar{c}}$$

The dividing point between vortices 2 and 3 (fig. 13a) was obtained from the inflection point on the span loading as recommended by Rossow (ref. 12). As can be seen, the comparison between the vortex-lattice theory and the experiment is excellent for vortices 2 and 3. It is believed that the measured strength of vortex 1 is lower than the theory because the vortex-lattice theory ignores the effect of the fuselage on the span loading. Apparently, the lift carry-over across the fuselage in the experiment leads to a weaker flap-inboard vortex than predicted by the theory for the wing alone. An adjusted span loading that takes into account the measured strength of the vortices is shown as a dashed curve in figure 13.

With the 30°/30° configuration (fig. 13b), good agreement was found for the outboard vortices (3 and 5). Exact agreement would be achieved by moving the dividing point from $\bar{y} = 0.90$ to 0.94; however, as discussed above, there is some uncertainty in the measured strengths of these vortices because of the axisymmetric model. The measurements indicate lower lift on the inboard flap and, as before, better lift carry-over across the fuselage when compared with the vortex-lattice theory for the wing alone.

SUMMARY AND CONCLUSIONS

Presented herein is a technique for experimentally analyzing complex aircraft wakes. First, extensive measurements were made of two components of velocity in a plane downstream of the wake generating model. These vortex wakes were then modeled by a superposition of axisymmetric vortices with finite cores. Good agreement was achieved between the analytical model and the measured velocities everywhere except where the vortices were in close proximity to each other. It is believed that the use of axisymmetric vortices to model the wake is inappropriate when vortices are about to merge. Finally, estimates of vortex strengths made from the span loadings calculated by vortex-lattice theory were also in good agreement with the present measurements in those regions where vortex-lattice theory would be expected to be valid. Therefore, it can be concluded that the superposition of axisymmetric vortices is a useful model for analyzing multiple vortex wakes. Although the analysis procedure was successfully completed for both configurations used in the present study, it was quite tedious for the configuration that contained six vortices per side. The analysis could be expedited by developing a least-square procedure to simultaneously evaluate all of the vortices.

Measurements made to determine the effect of the landing gear on the 30°/0° configuration indicated no significant effect on the vertical velocity distribution. Additional velocity measurments at greater downstream distance than used in the present tests will be required to analyze the effect of the landing gear.

REFERENCES

1. Gessow, A.: Aircraft Wake Turbulence Minimization by Aerodynamic Means. 6th Conference on Aerospace and Aeronautical Meteorology, El Paso, Texas, Nov. 12-14, 1974.

2. NASA Symposium on Wake Vortex Minimization. NASA SP-409, Feb. 25-26, 1976.

3. Rossow, V. J.: Convective Merging of Vortex Cores in Lift-Generated Wakes. AIAA Paper 76-415, July 14-16, 1976.

4. Corsiglia, V. R.; Rossow, V. J.; and Ciffone, D. L.: Experimental Study of the Effect of Span Loading on Aircraft Wakes. NASA TMX-62, 431, May 1975.

5. Ciffone, D. L.; and Lonzo, C., Jr.: Flow Visualization of Vortex Interactions in Multiple Vortex Wakes Behind Aircraft. NASA TM X-62, 459, June 1975.

6. Corsiglia, V. R.; and Dunham, R. E.: Aircraft Wake-Vortex Minimization by Use of Flaps. NASA SP-409, Feb. 1976, pp. 303-336.

7. Barber, M. R.; Gatlin, D. H.; Hastings, E.C., Jr.; Tymczyszyn, J. J.: Vortex Attenuator Flight Experiments. NASA SP-409, Feb. 1976, pp. 338ff.

8. Corsiglia, V. R.; Schwind, R. G.; and Chigier, N.A.: Rapid-Scanning Three-Dimensional, Hot-Wire Anemometer Surveys of Wing-Tip Vortices. J. Aircraft, vol. 10, no. 12, Dec. 1973, pp. 752-757.

9. Orloff, K. L.; Corsiglia, V.R.; Biggers, J.C.; and Ekstedt, T.W.; Investigating Complex Aerodynamic Flows with a Laser Velocimeter, the Accuracy of Flow Measurements by by Laser Doppler Methods. Proceedings of the LDA-Symposium, Copenhagen, 1975, P. O. Box 70, DK-2740 Skovlunde, Denmark, pp. 624-643. (See also NASA TM X-73, 171, Sept. 1976.)

10. Grant, G. R.; and Orloff, K. L.: A Two-Color, Dual Beam Backscatter Laser Doppler Velocimeter. NASA TM X-62,254, March 1973.

11. Hough, G.: Remarks on Vortex-Lattice Methods. AIAA J. Aircraft, vol. 10, no. 5, May 1973, pp. 314-317.

12. Rossow, V. J.: On the Inviscid Rolled-Up Structure of Lift Generated Vortices. AIAA J. Aircraft, vol. 10, no. 11, Nov. 1973, pp. 647-650.

TABLE 1.– MODEL DIMENSIONS, WIND-TUNNEL AND TEST CONDITIONS

Generator Model (Boeing 747)	
Wing	
Span, cm (in.)	179 (70.5)
Root incidence	+2°
Tip incidence	–2°
Area, m^2 (ft^2)	0.459 (4.94)
Average chord, cm (in.)	25.6 (10.1)
Aspect ratio	7
Horizontal stabilizer	0°
Wind-tunnel and Test conditions	
U_∞, m/s (ft/sec)	14 (46)
Reynolds number based on average chord	$2.5X10^5$
Lift coefficient	1.2
Angle of Attack	
Flaps 30°/0°	7°
Flaps 30°/30°	2°

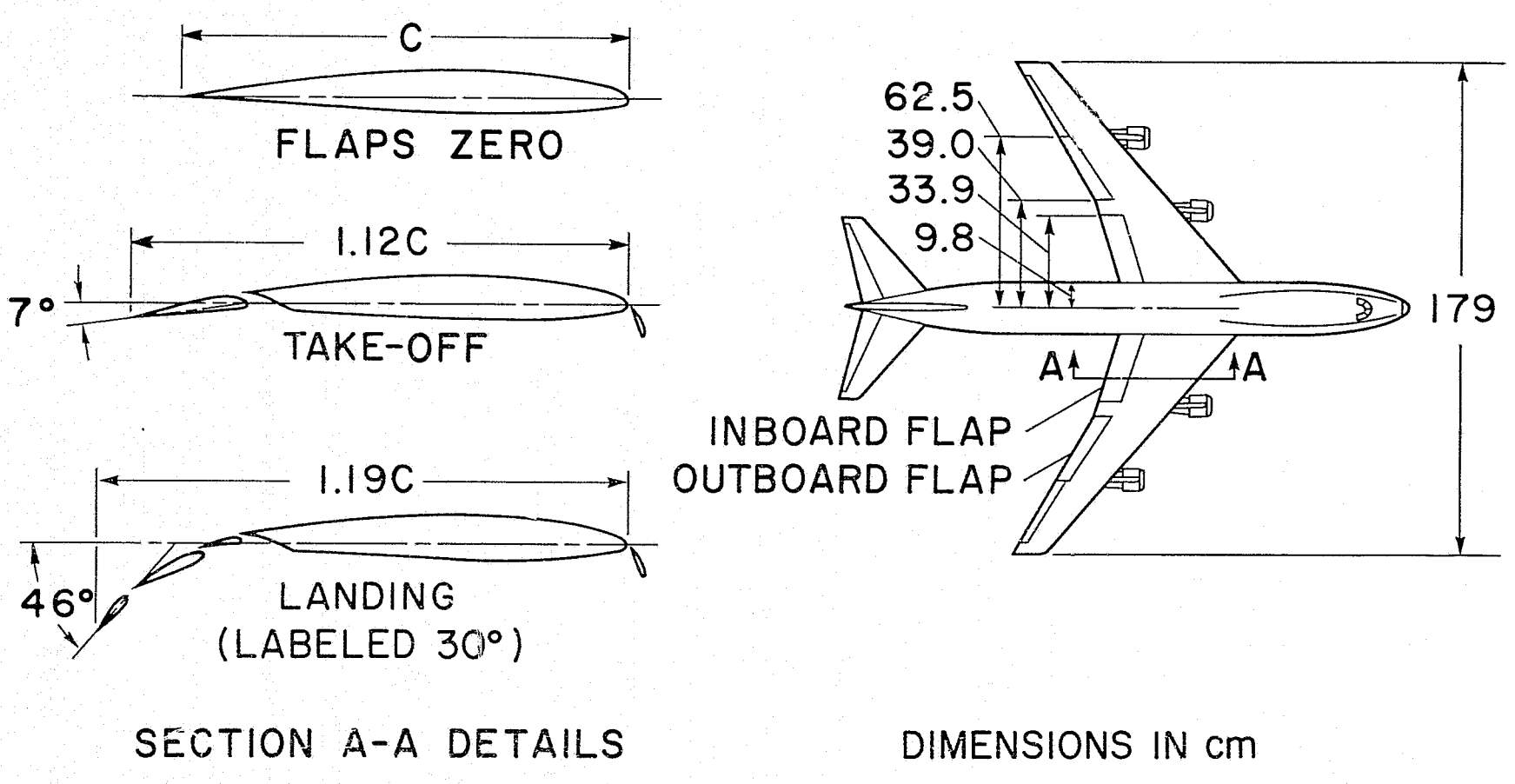

Figure 1. — Geometric details of the B747 subsonic transport model.

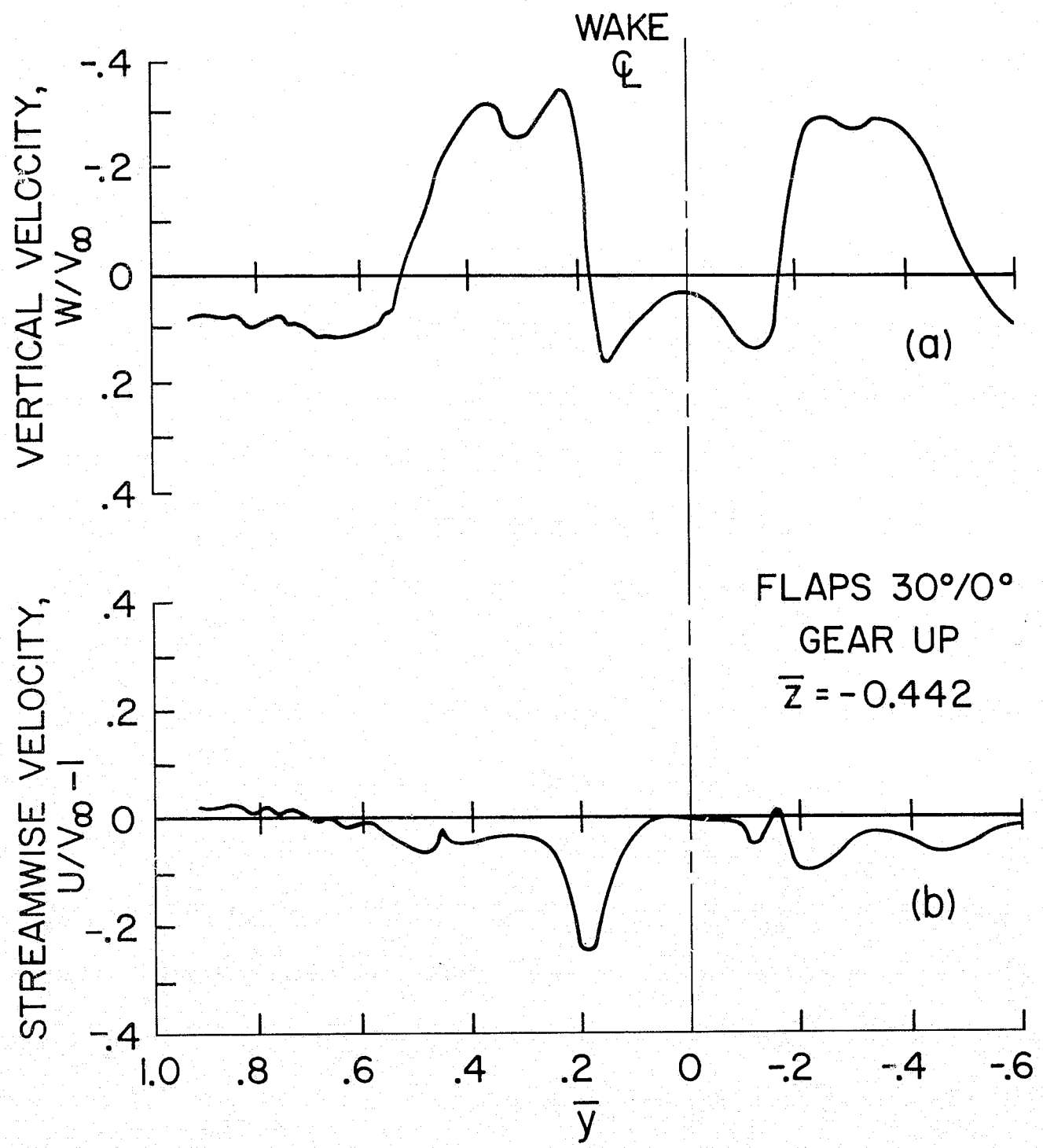

(a) Vertical velocity component.

(b) Streamwise velocity component.

Figure 2. -- Example of laser velocimeter data after smoothing and replotting. Flaps 30°/0°, gear up, $\bar{z} = -0.442$.

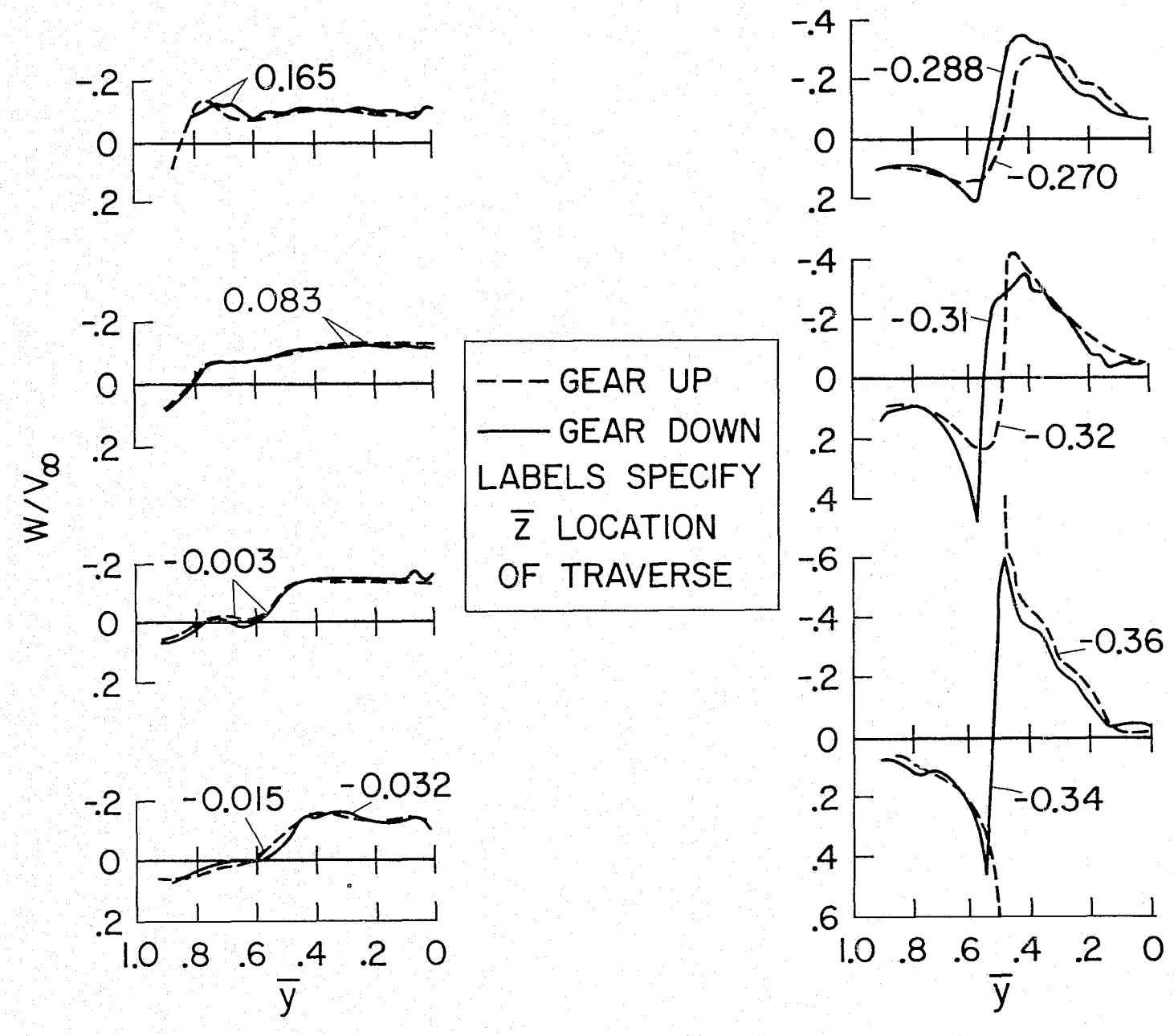

Figure 3. - Effect of the landing gear on the variation of vertical velocity. Flaps 30°/0°.

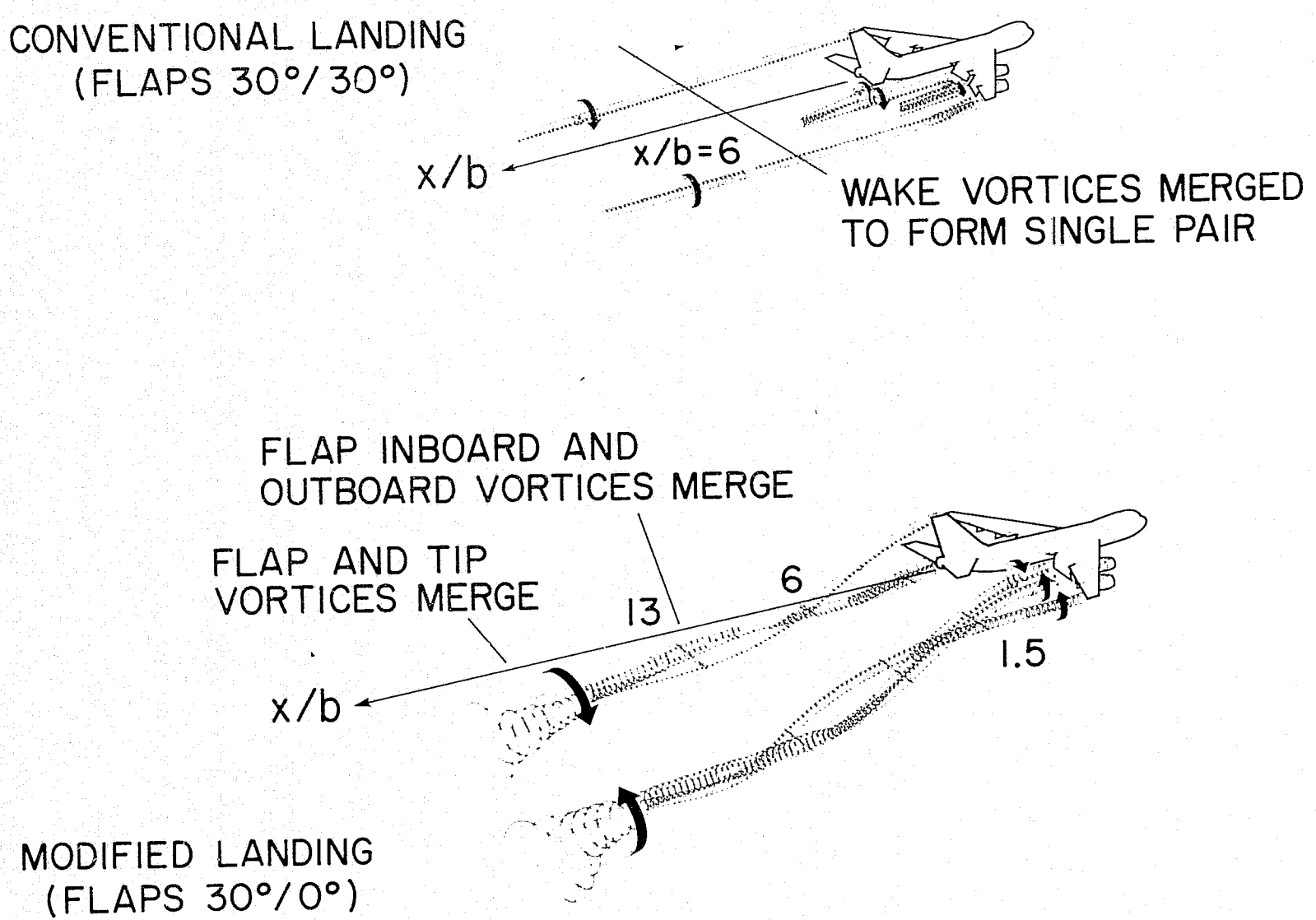

Figure 4. – Summary of vortex trajectories from flow visualization studies.

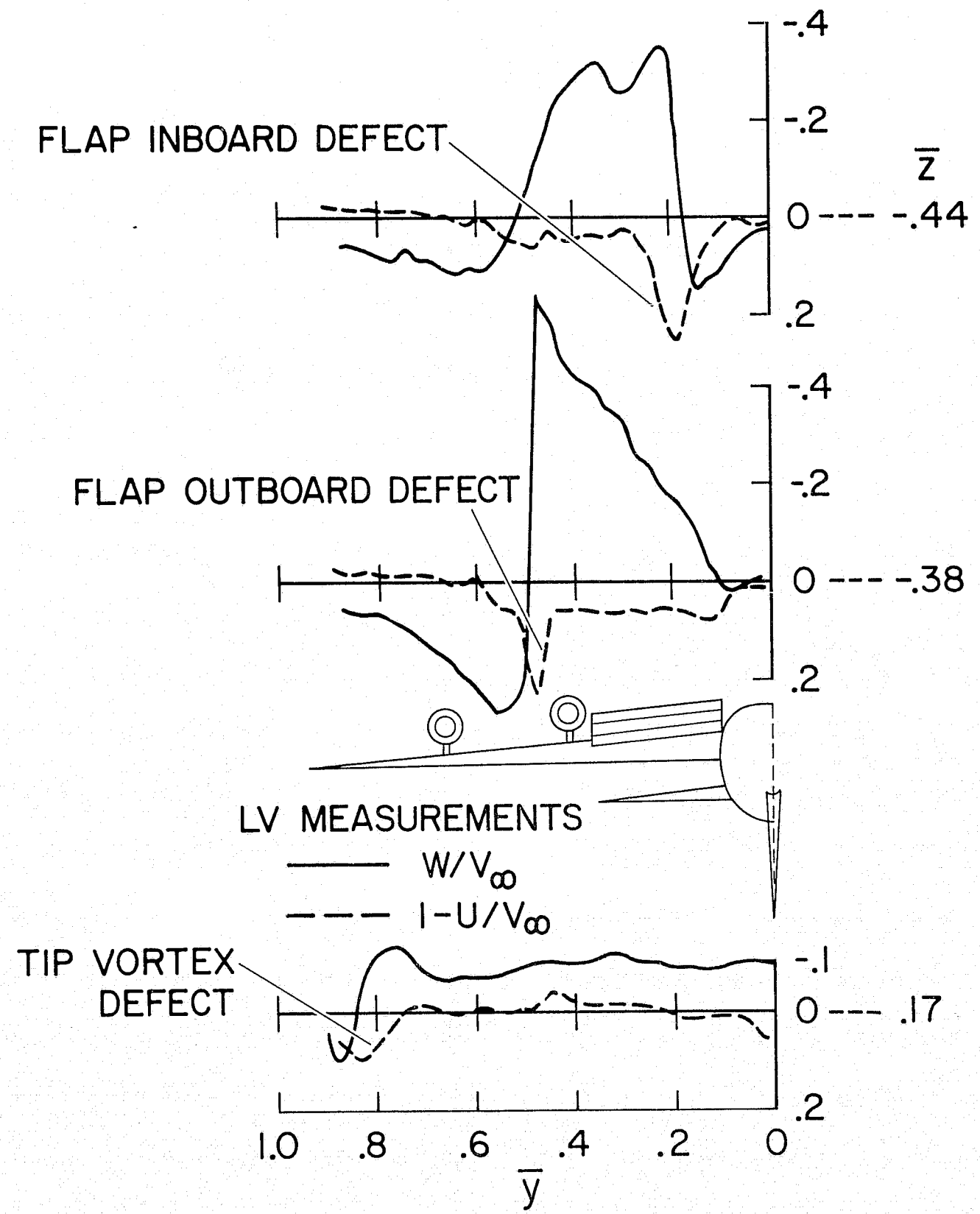

Figure 5. Variation of vertical and streamwise velocity distributions for lateral traverses through each vortex center. Flaps 30°/0°, gear up.

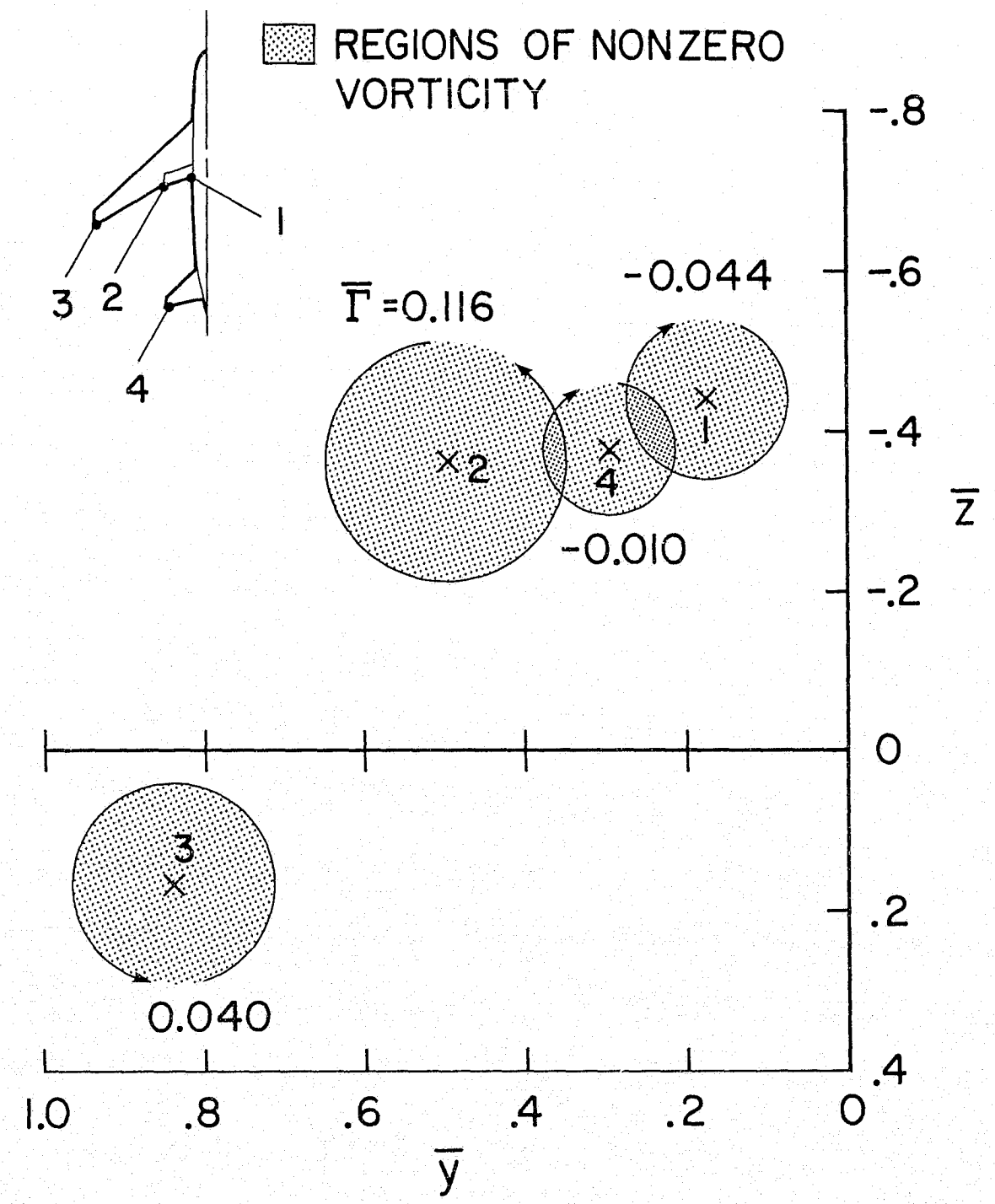

Figure 6. – Vortex locations, strengths and regions of varying circulation resulting from analysis of measured velocity. Flaps 30°/0°, gear up.

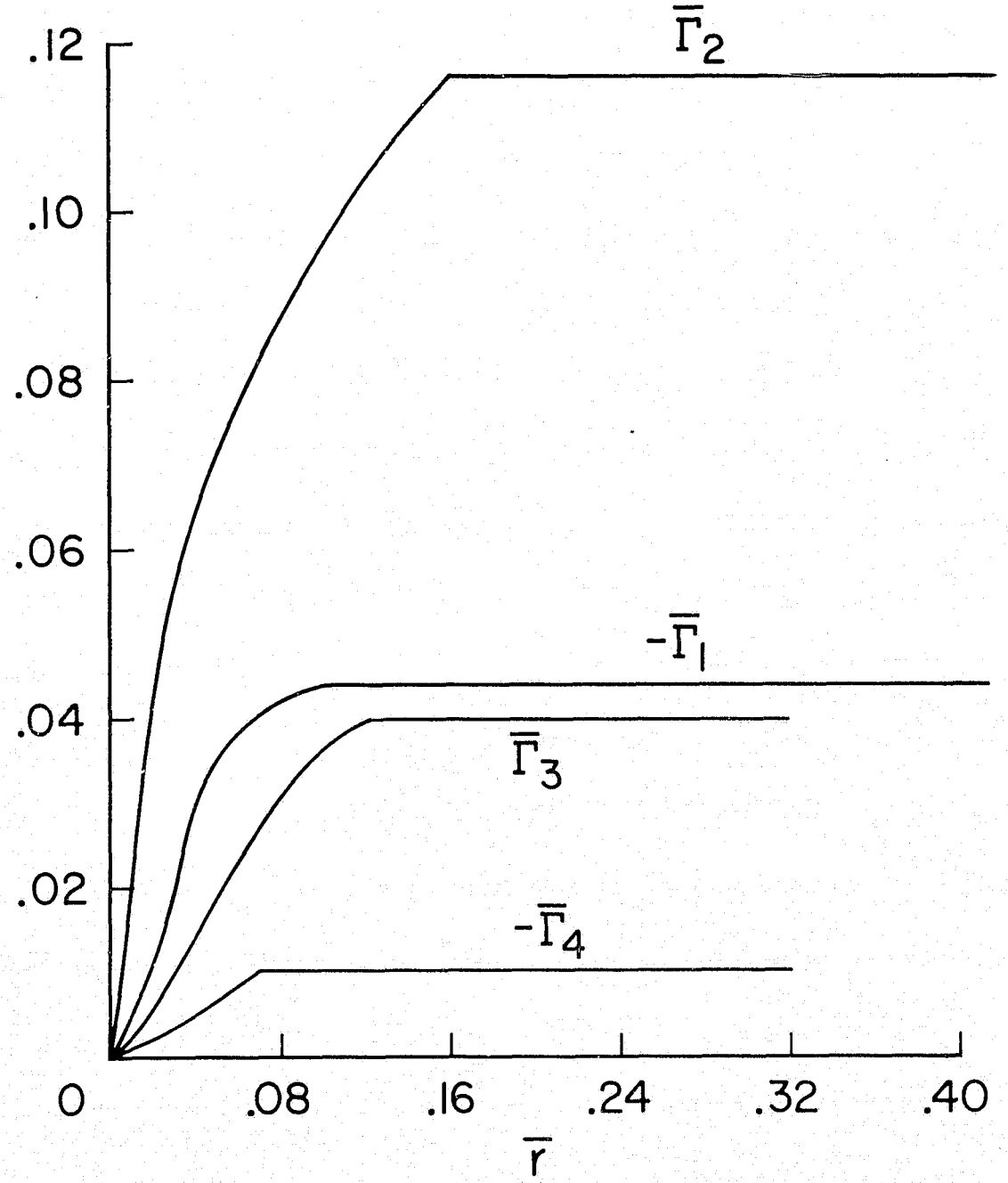

Figure 7. Circulation distributions resulting from analysis of measured velocity. Flaps 30°/0°, gear up.

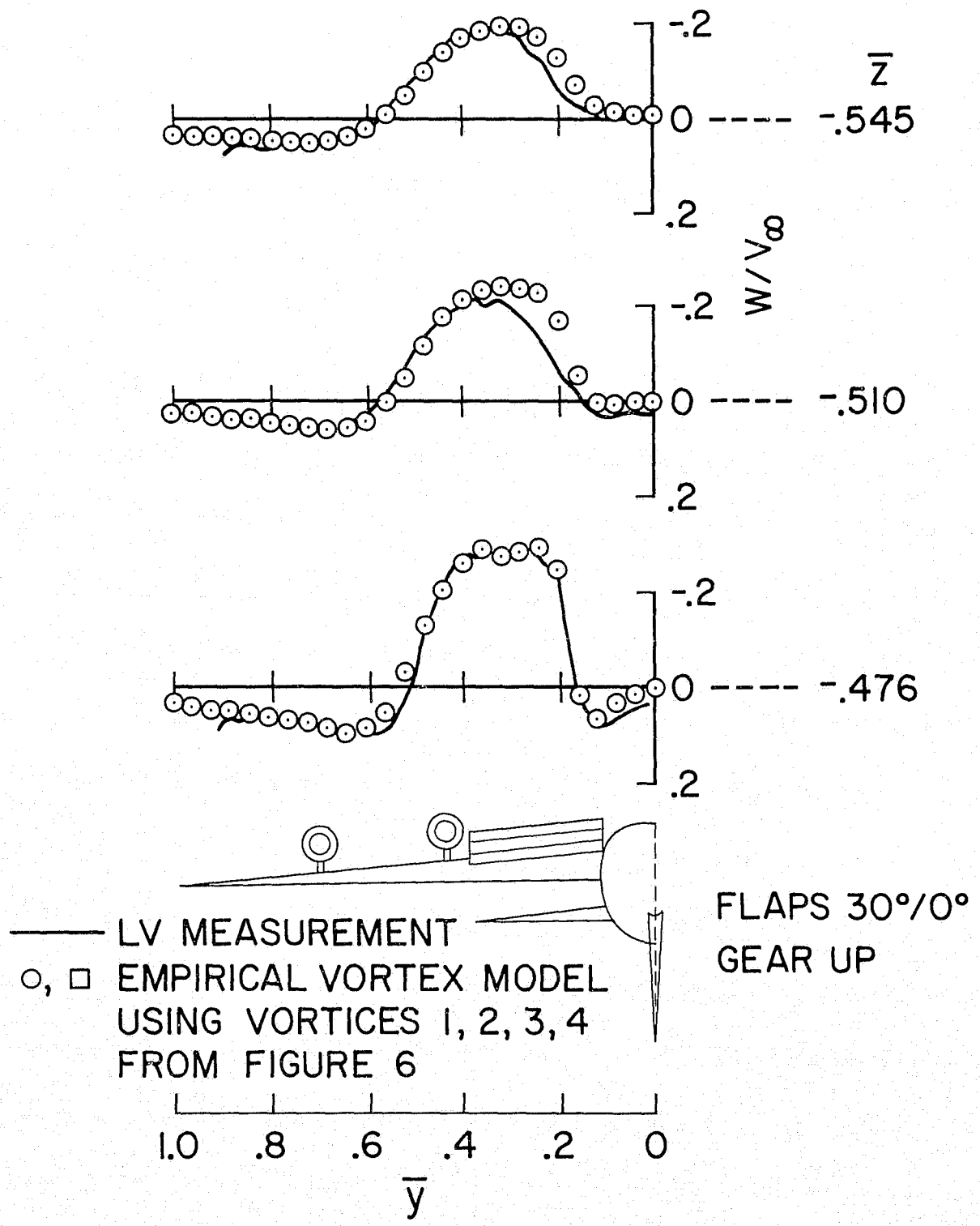

(a) $\bar{z} = -0.545, -0.510, -0.476$.

Figure 8. – Comparison between measured vertical velocities and the axisymmetric vortex model using the vortices shown on figures 6 and 7. Flaps 30°/0°, gear up.

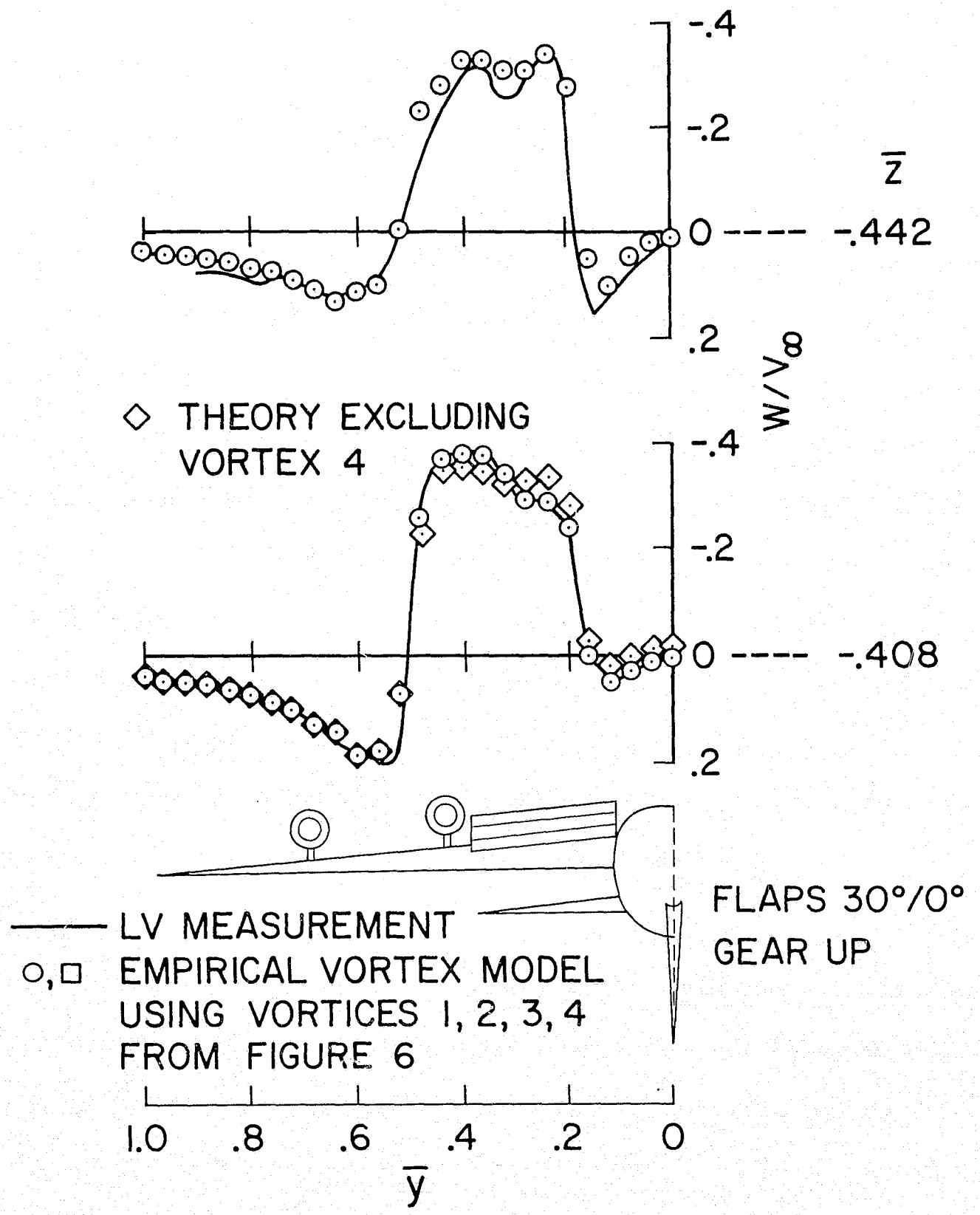

(b) $\bar{z} = -0.442, -0.408$.

Figure 8. Continued.

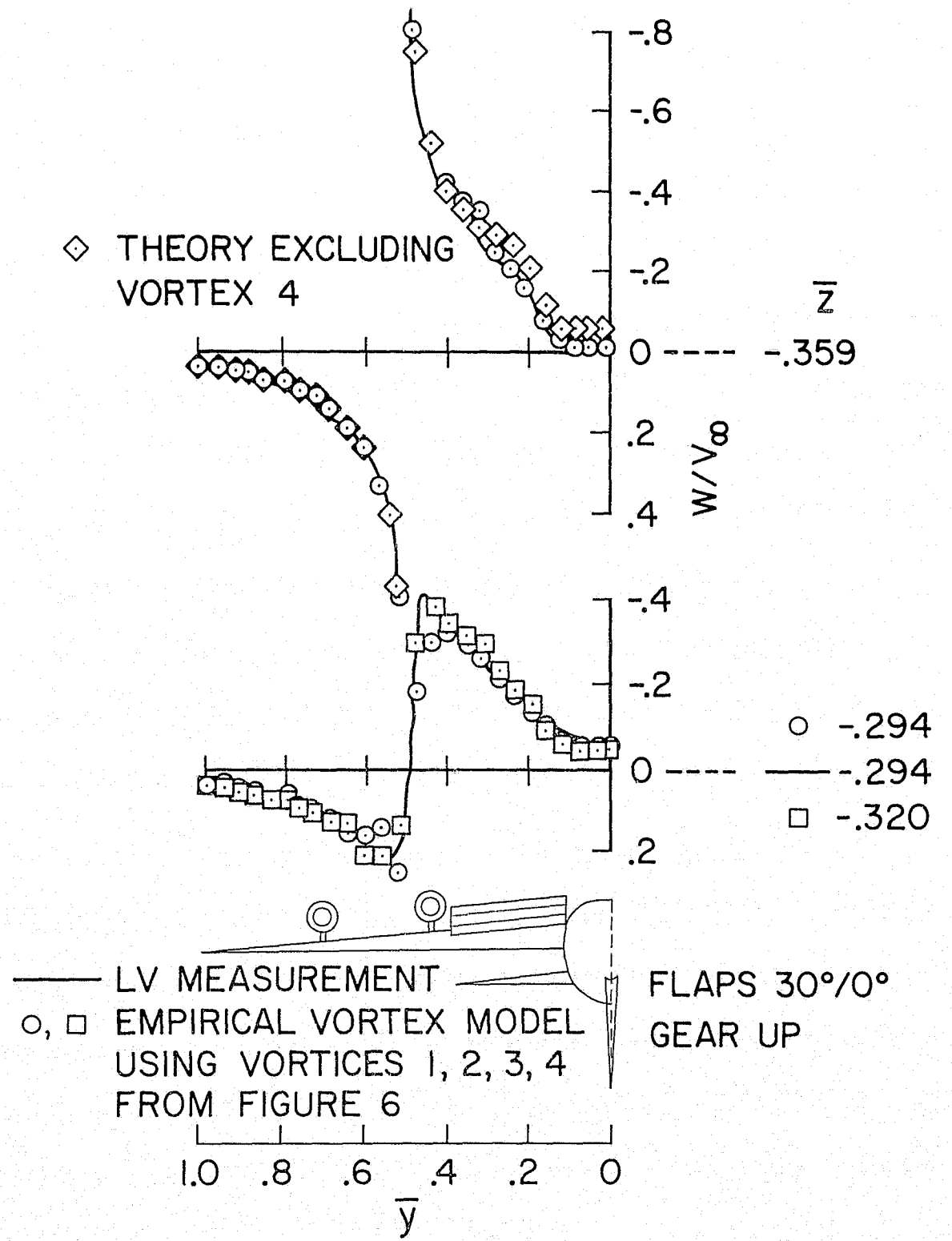

(c) $\bar{z} = -0.359, -0.294$.

Figure 8. — Continued.

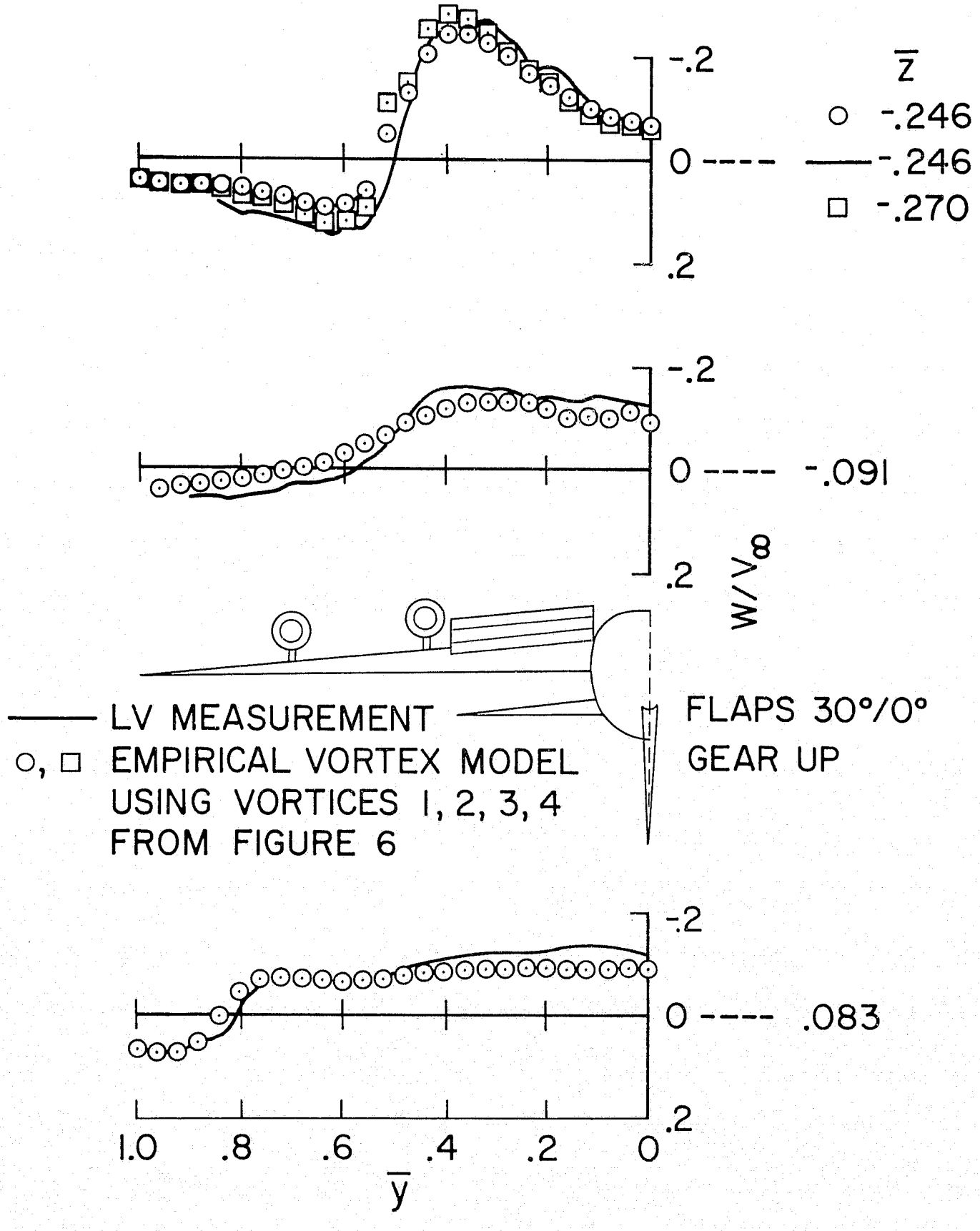

(d) $\bar{z} = -0.246, -0.091, +0.083$.

Figure 8. Continued.

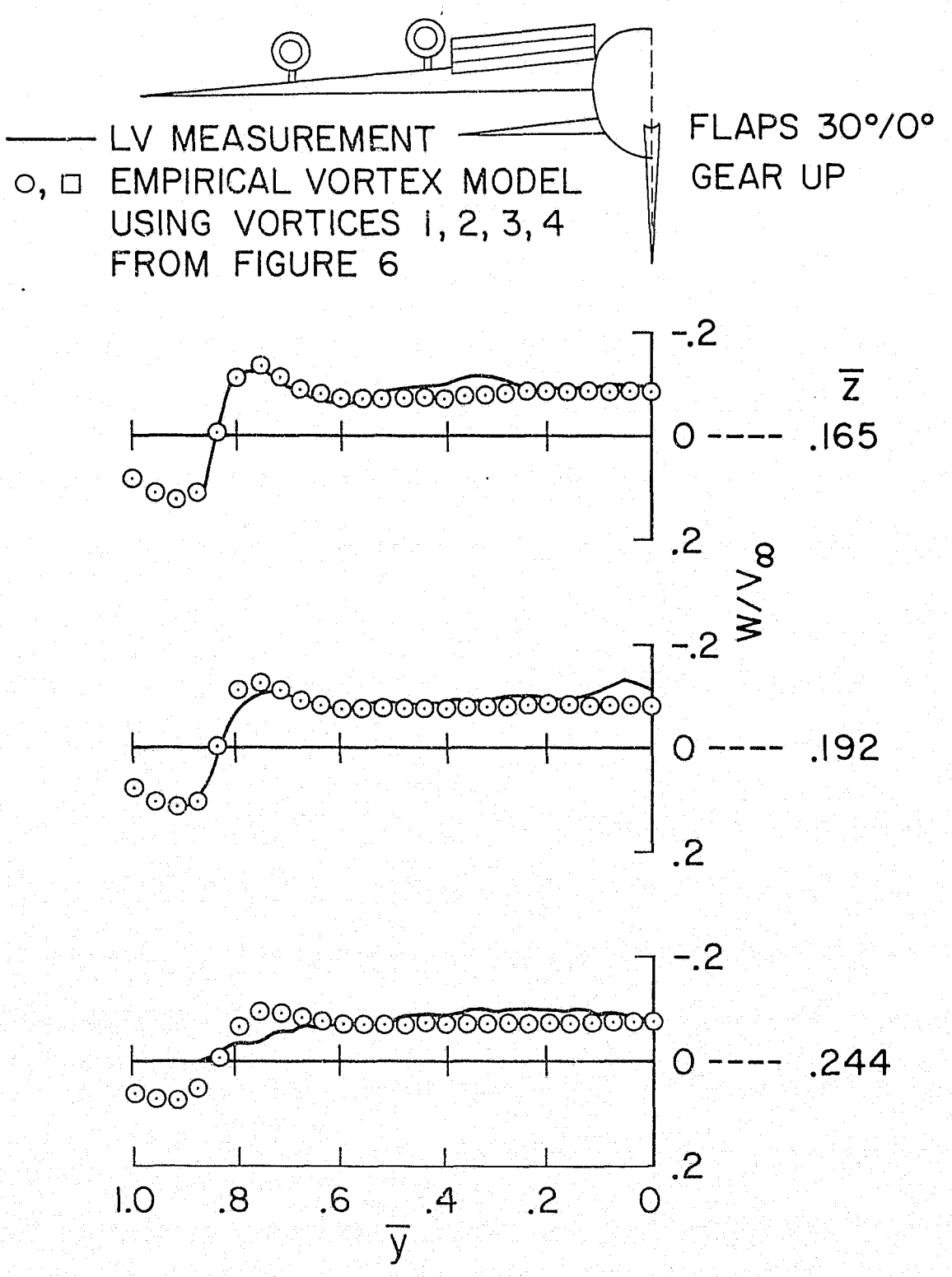

(e) $\bar{z}$ = +0.165, +0.192, +0.244.

Figure 8. Concluded.

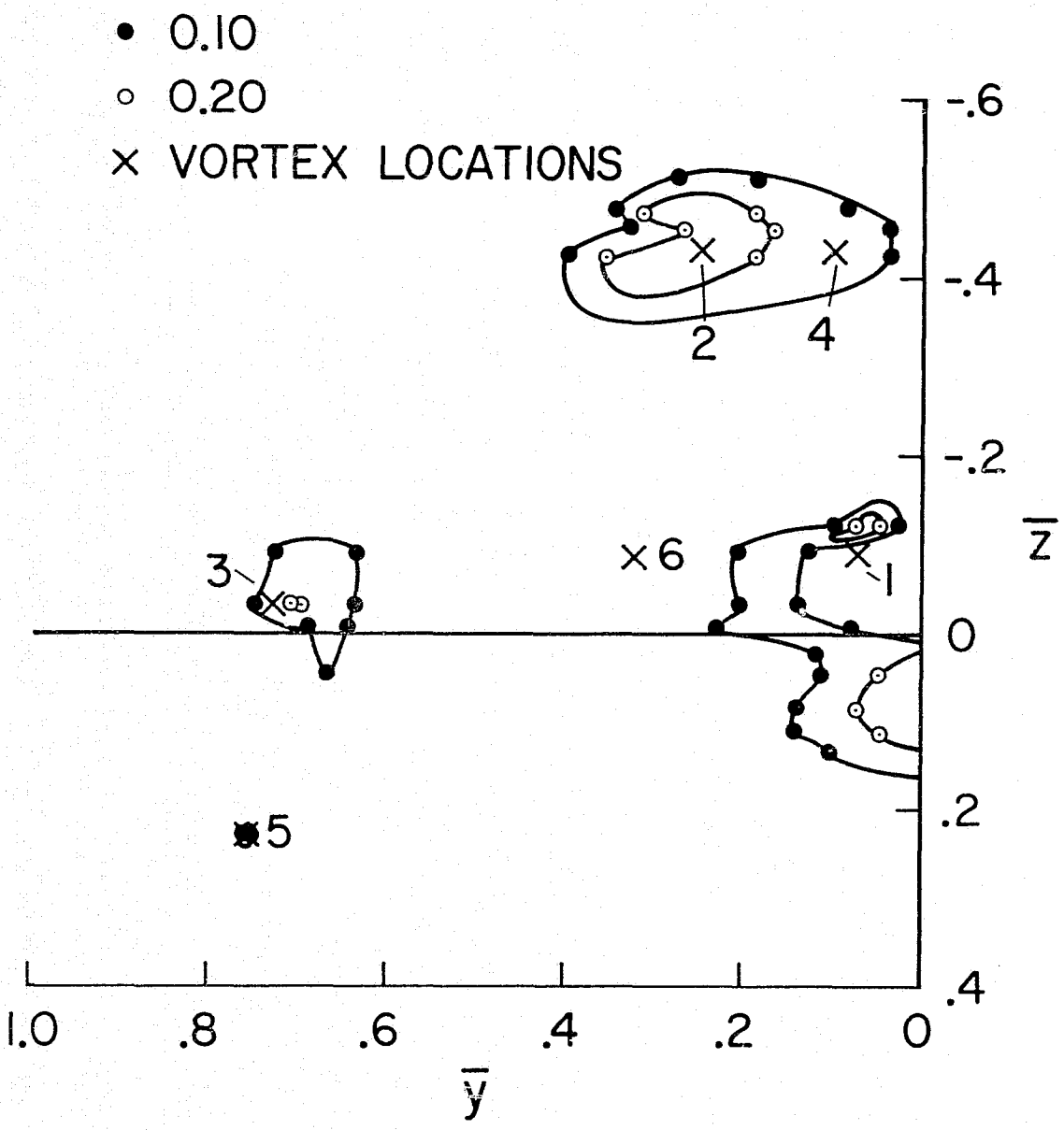

Figure 9. - Regions of significant streamwise velocity defect and the locations of the vortices from the analysis of measured velocities. Flaps 30°/30°, gear up.

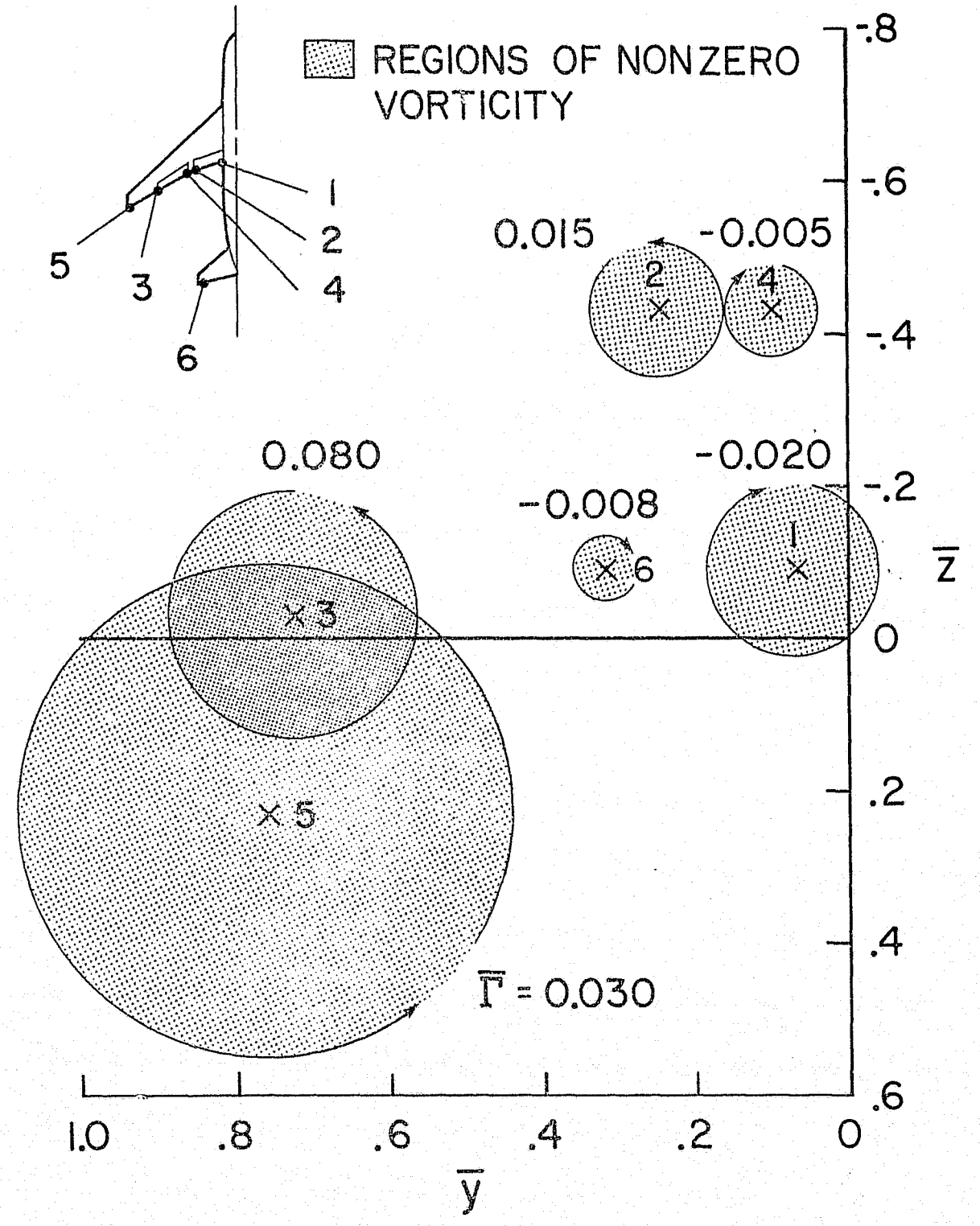

Figure 10. Vortex locations, strengths, and regions of varying circulation resulting from analysis of measured velocities. Flaps 30°/30°, gear up.

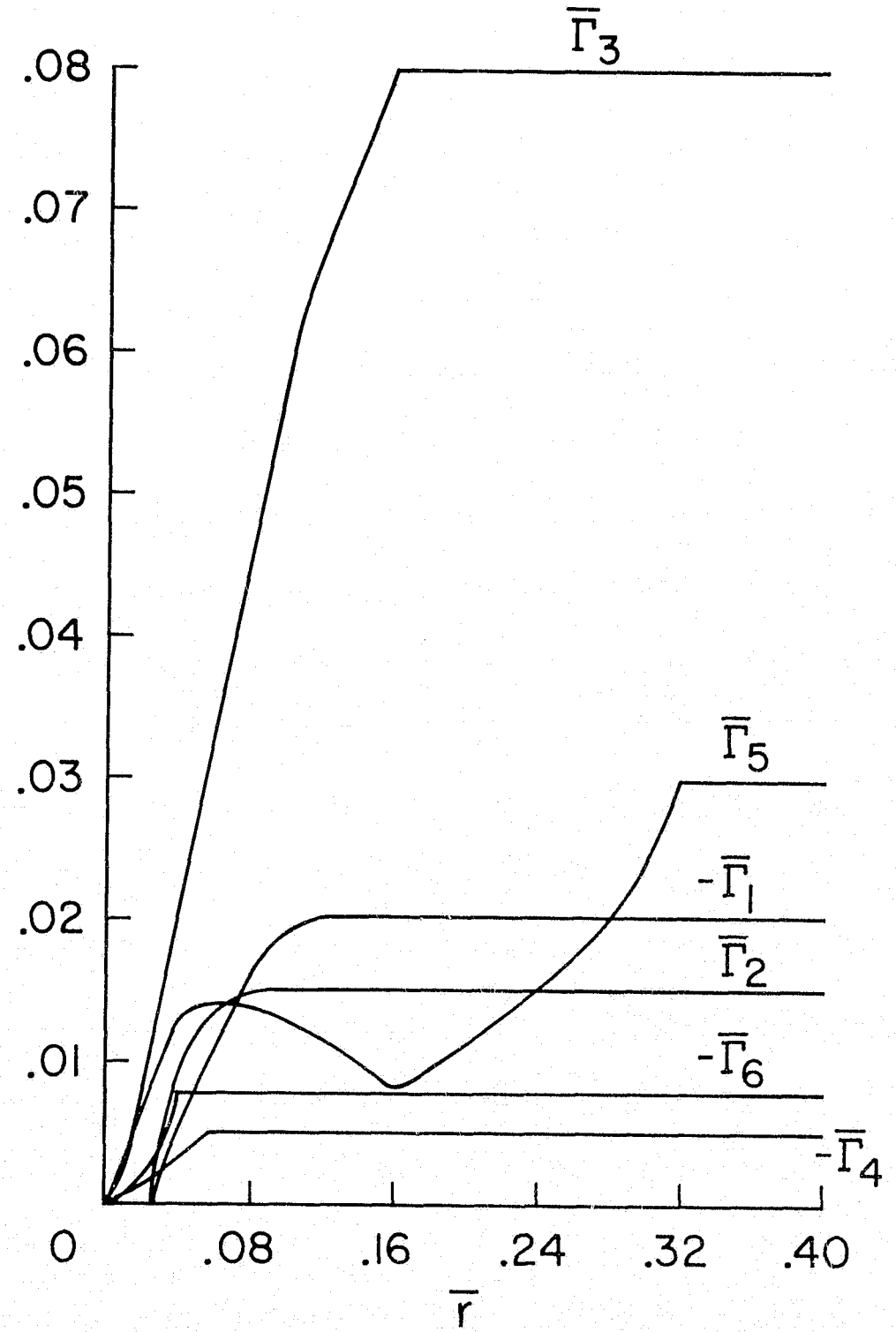

Figure 11. Circulation distributions resulting from analysis of measured velocities. Flaps 30°/30°, gear up.

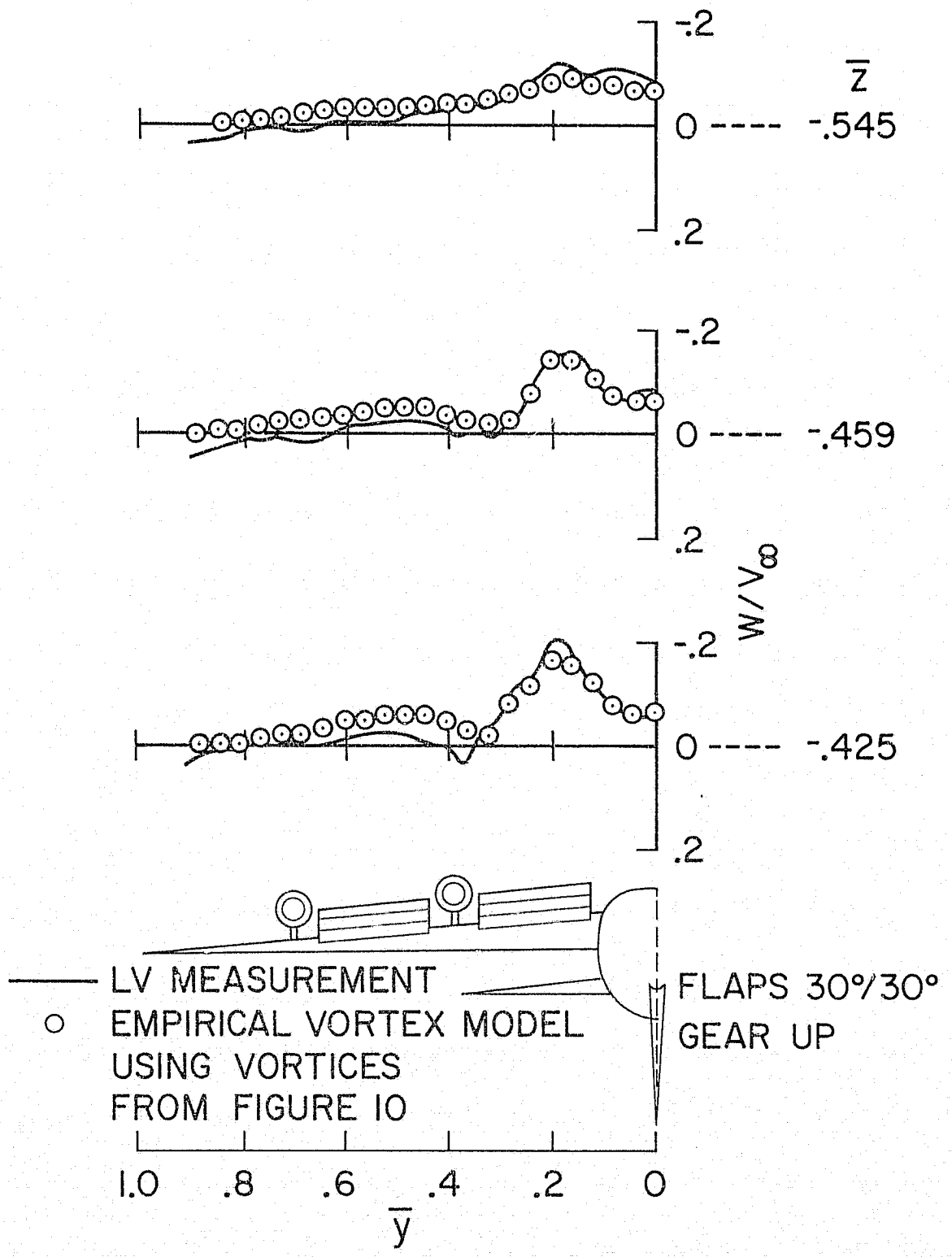

(a) $\bar{z}$ = -0.545, -0.459, -0.425.

Figure 12. Comparison between measured vertical velocities and the axisymmetric vortex model using the vortices shown on figures 11 and 12. Flaps 30°/30°, gear up.

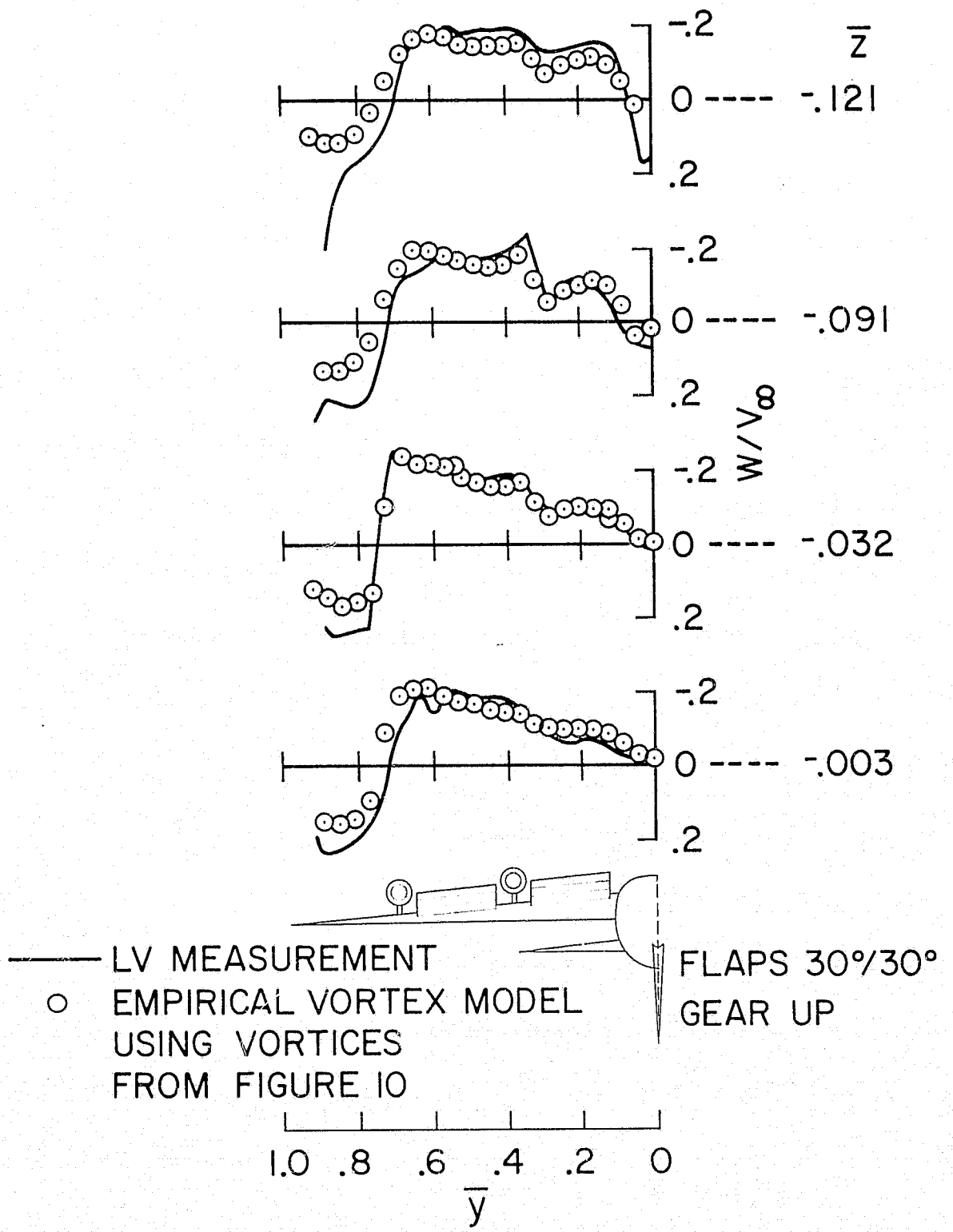

(b) $\bar{z} = -0.121, -0.091, -0.032, -0.003$.

Figure 12. Continued.

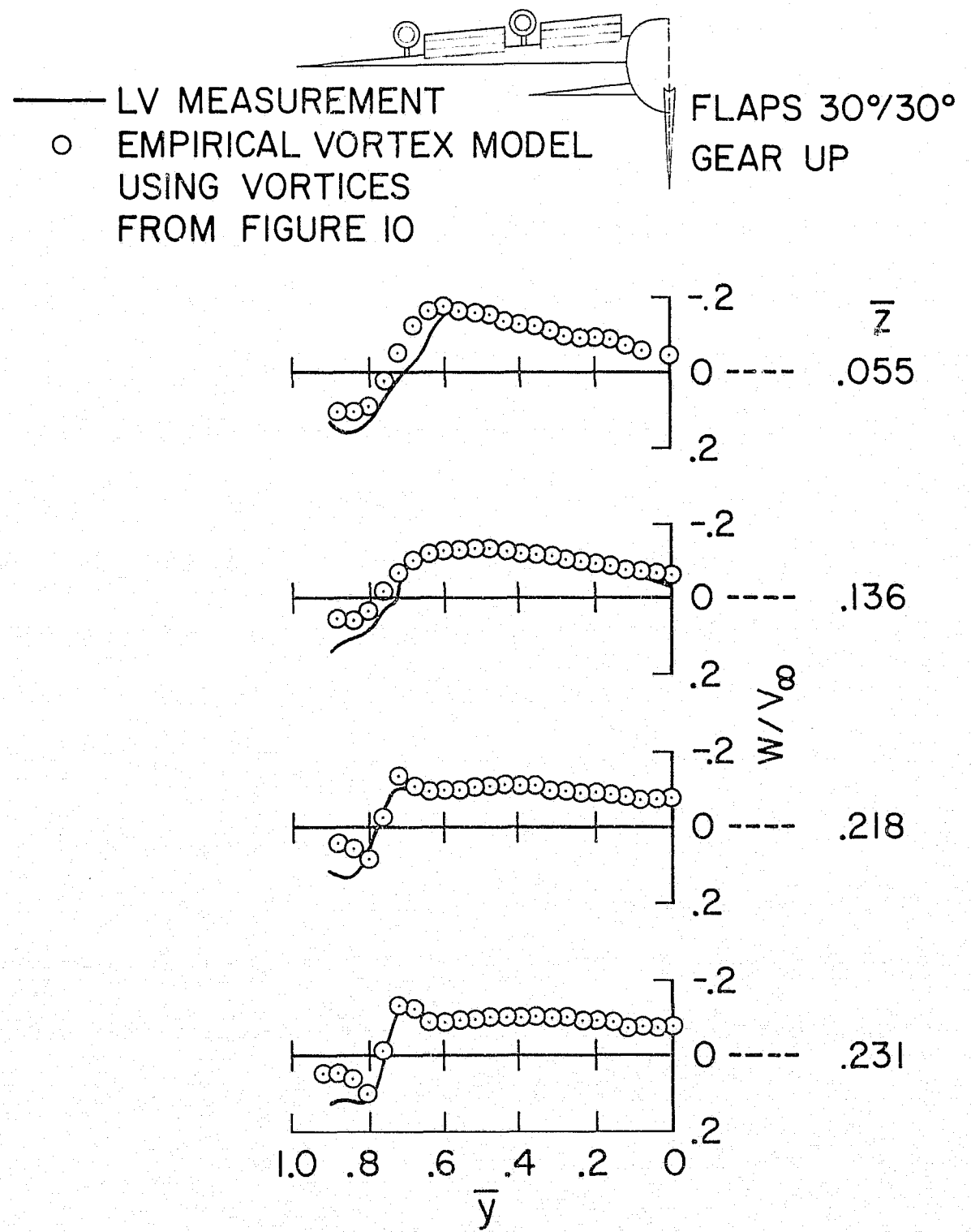

(c) $\bar{z} = +0.055, +0.136, +0.218, +0.231$.

Figure 12. – Continued.

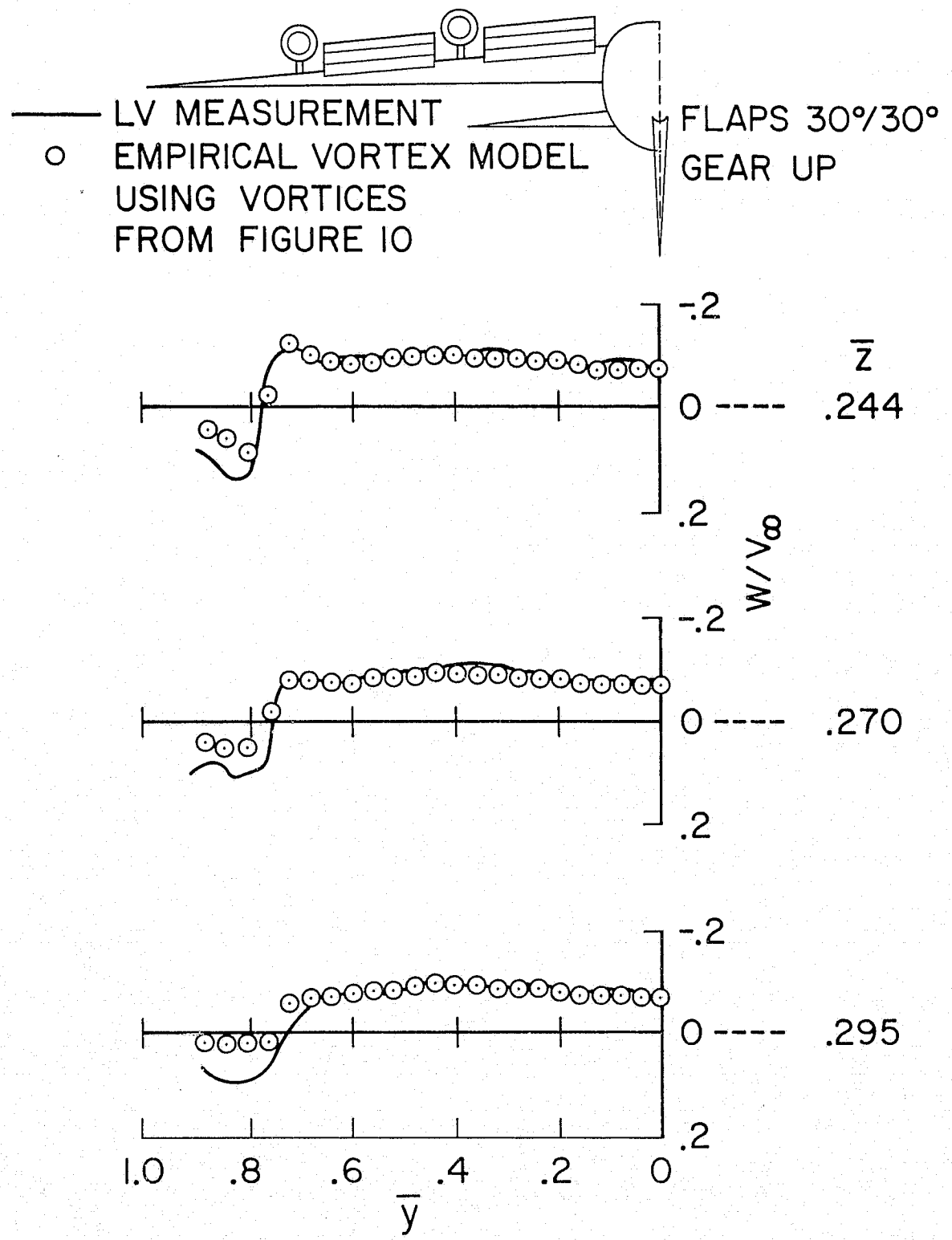

(d) $\bar{z} = +0.244, +0.270, +0.295$.

Figure 12. Concluded.

MAX VORTEX CIRCULATION, $\bar{\Gamma}$

	1	2	3
VORTEX LATTICE THEORY	-0.064	0.116	0.042
MEASURED	-0.044	0.116	0.040

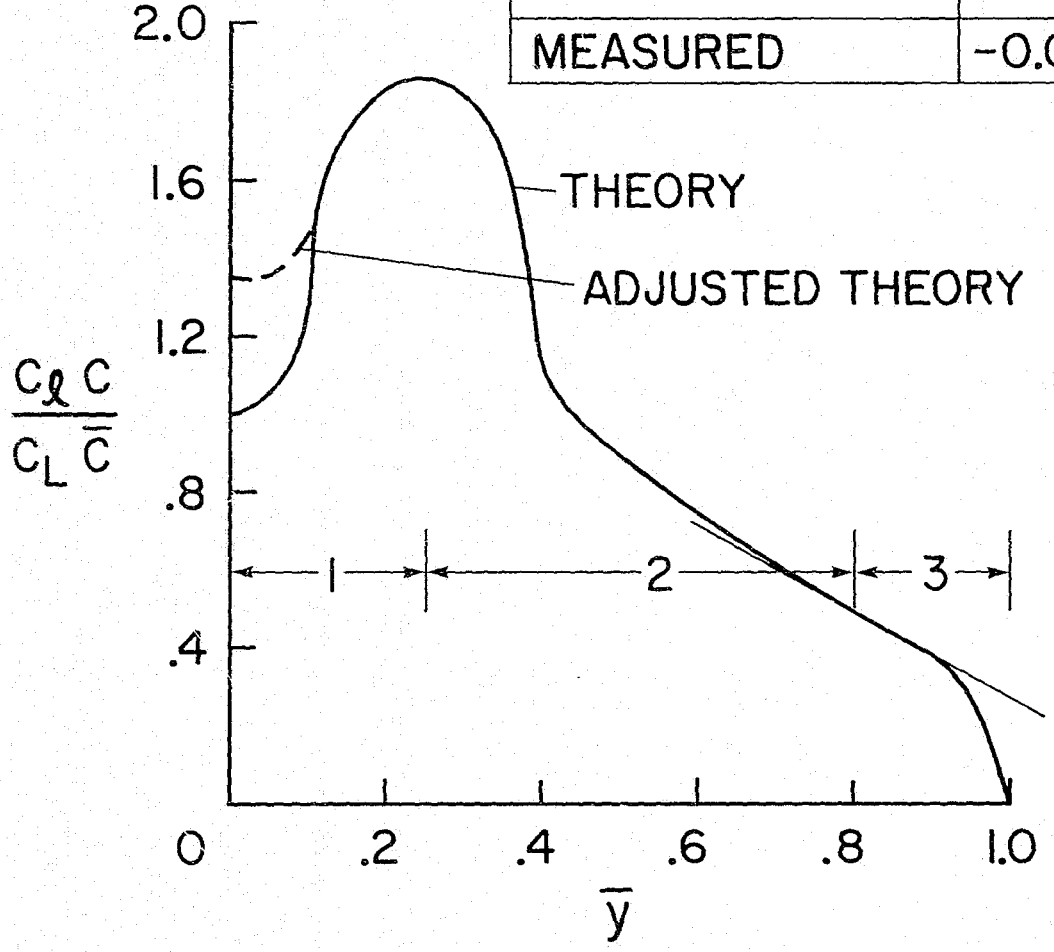

(a) Flaps 30°/0°, $\alpha = 7°$.

Figure 13. -- Comparison of maximum vortex circulation from vortex lattice theory and the axisymmetric model for the measured velocities. Gear up.

MAX VORTEX CIRCULATION, $\overline{\Gamma}$

	1	2	3	4	5
LIFTING SURFACE THEORY	-0.072	0.060	0.084	-0.029	0.025
MEASURED	-0.020	0.015	0.080	-0.005	0.030

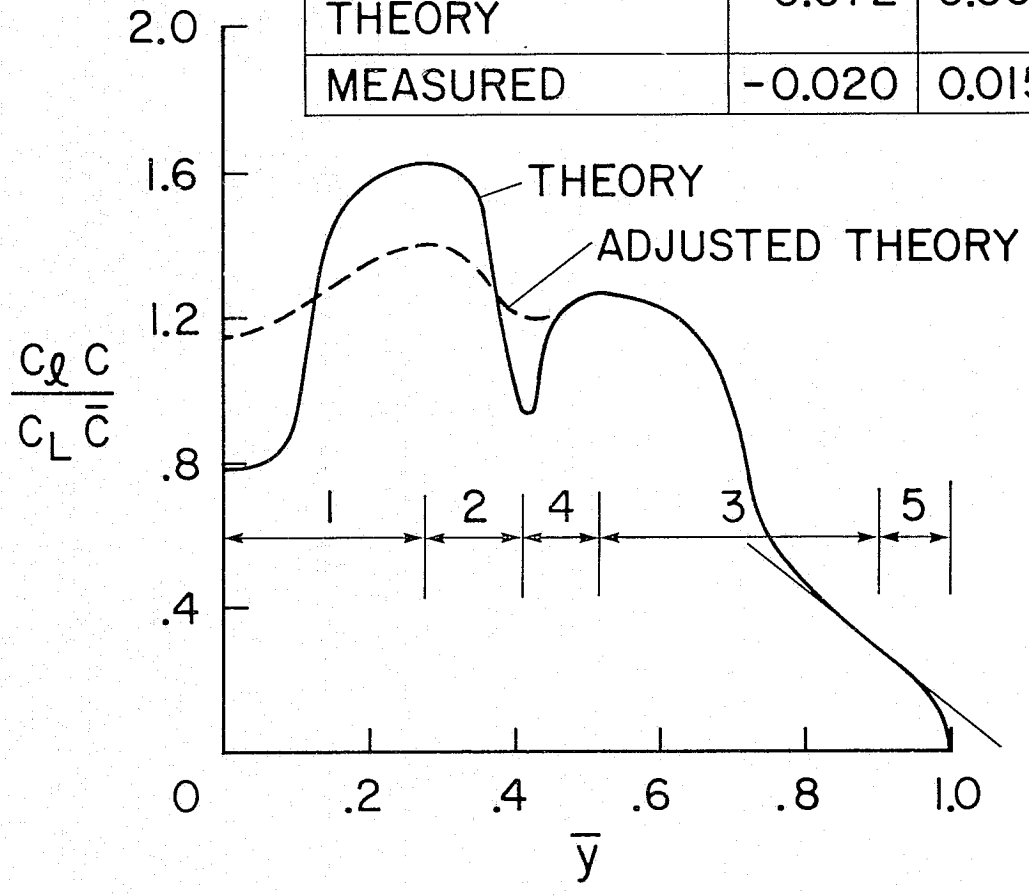

(b) Flaps 30°/30°, $\alpha = 2°$.

Figure 13. Concluded.